AD-A053 847 NAVAL RESEARCH LAB WASHINGTON D C F/G 20/9
WHYRAC, A NEW MODULAR ONE-DIMENSIONAL EXPLODING WIRE CODE.(U)
FEB 78 D G COLOMBANT, M LAMPE, H W BLOOMBERG
UNCLASSIFIED NRL-MR-3726 SBIE-AD-E000 145 NL

END
DATE FILMED
6 -78
DDC

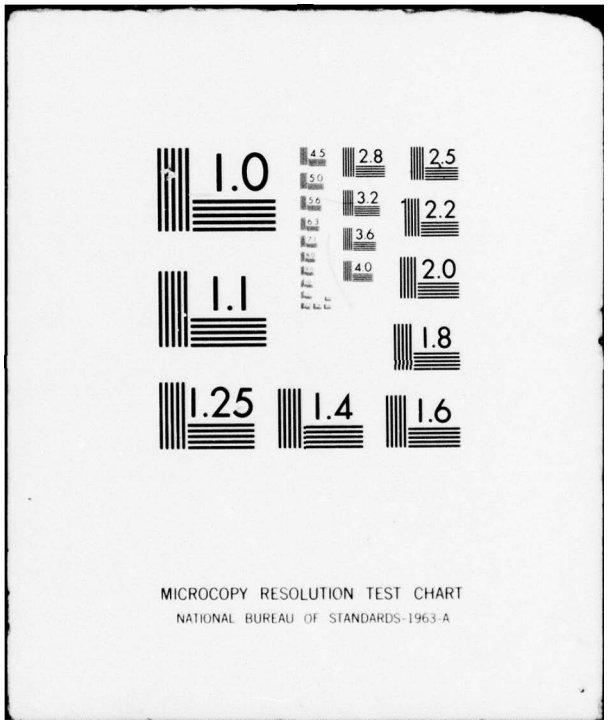
1.0
1.1
1.25
1.4
1.6
1.8
2.0
2.2
2.5
2.8
3.2
3.6
4.0
4.5
5.0
5.6
6.3
MICROCOPY RESOLUTION TEST CHART
NATIONAL BUREAU OF STANDARDS-1963-A

NRL Memorandum Report 3726

WHYRAC, A New Modular One-Dimensional Exploding Wire Code

D. G. COLOMBANT AND M. LAMPE

Plasma Dynamics Branch
Plasma Physics Division

and

H. W. BLOOMBERG
Science Applications, Inc.
McLean, Virginia 22209

February 1978

This research was sponsored by the Defense Nuclear Agency under Subtask T99QAXLB203, work unit 12 and work unit title, Advanced Concepts Theory.

NAVAL RESEARCH LABORATORY
Washington, D.C.

SECURITY CLASSIFICATION OF THIS PAGE (When Data Entered)

REPORT DOCUMENTATION PAGE

READ INSTRUCTIONS BEFORE COMPLETING FORM

1. REPORT NUMBER: NRL ~~Memorandum Report~~ -MR- 3726
2. GOVT ACCESSION NO.
3. RECIPIENT'S CATALOG NUMBER

4. TITLE (and Subtitle): WHYRAC, A NEW MODULAR ONE-DIMENSIONAL EXPLODING WIRE CODE.
5. TYPE OF REPORT & PERIOD COVERED: Interim report on a continuing NRL problem.
6. PERFORMING ORG. REPORT NUMBER

7. AUTHOR(s): B. G./Colombant, ~~M.~~ MARTIN /Lampe, ~~M.~~ H. W./Bloomberg, SAI
8. CONTRACT OR GRANT NUMBER(s)

9. PERFORMING ORGANIZATION NAME AND ADDRESS: Naval Research Laboratory, Washington, D.C. 20375
10. PROGRAM ELEMENT, PROJECT, TASK AREA & WORK UNIT NUMBERS: NRL Problem H02-26K; DNA Subtask T99QAXLB203

11. CONTROLLING OFFICE NAME AND ADDRESS: Defense Nuclear Agency, Washington, D.C. 20305
12. REPORT DATE: February 1978
13. NUMBER OF PAGES: 34

14. MONITORING AGENCY NAME & ADDRESS (if different from Controlling Office)
15. SECURITY CLASS. (of this report): UNCLASSIFIED
15a. DECLASSIFICATION/DOWNGRADING SCHEDULE

16. DISTRIBUTION STATEMENT (of this Report)

Approved for public release; distribution unlimited.

17. DISTRIBUTION STATEMENT (of the abstract entered in Block 20, if different from Report)

18. SUPPLEMENTARY NOTES

This research was sponsored by the Defense Nuclear Agency under Subtask T99QAXLB203, work unit 12 and work unit title, Advanced Concepts Theory.

19. KEY WORDS (Continue on reverse side if necessary and identify by block number)

Z-pinch
Wire produced plasma
Numerical MHD

20. ABSTRACT (Continue on reverse side if necessary and identify by block number)

A new one-dimensional code, WHYRAC, intended to provide a comprehensive treatment of exploding wires and wire arrays, is described. The circuit equations treat the wire plasma in an exact way, rather than using a lumped circuit model. Great care has been taken in the Eulerian MHD treatment of plasma motion, resulting in an unusual combination of rapid running capability to handle density ranges spanning at least four orders of magnitude, and very accurate energy conservation in the overall circuit. The code is written in a modular and flexible way,

(Continues)

DD FORM 1 JAN 73 1473 EDITION OF 1 NOV 65 IS OBSOLETE
S/N 0102-014-6601

SECURITY CLASSIFICATION OF THIS PAGE (When Data Entered)

251 950

20. Abstract (Continued)

to permit continual upgrading, and extension to different elements, of the atomic physics and radiation transport packages. At present, a fairly simple, rapid-running model (one line per ionization level, localized treatment of radiation transport) is used to provide transport at each time step. A much more extensive, state-of-the-art, atomic/radiation code is used to generate output radiation spectra when required, and to benchmark the energy transport package. The report gives special attention to the treatment of numerical problems in WHYRAC.

CONTENTS

I. INTRODUCTION 1

II. THE MHD EQUATIONS 3

III. CIRCUIT EQUATION 9

IV. ATOMIC PHYSICS AND RADIATION 14

V. CONCLUSION 18

ACKNOWLEDGMENT 19

REFERENCES 20

WHYRAC, A NEW MODULAR ONE-DIMENSIONAL EXPLODING WIRE CODE

I. Introduction

The dynamic evolution of an exploding wire or an array of parallel-strung exploding wires depends in detail on at least three different types of physical phenomena: the magnetohydrodynamic fluid motion of the wire plasma, the coupling of the wire plasma to the driving electric circuit, and the atomic physics and radiative energetics of the high-Z plasma. These different classes of phenomena are intimately cross-coupled. For example, the plasma temperature/density profile depends sensitively on atomic excitation energy sources and sinks, radiative energy transport, and ohmic energy deposition by the external circuit, as well as on MHD phenomena such as compression and shocks. The circuit current depends on the plasma temperature/density profile, in a way that cannot consistently be modeled in terms of lumped circuit elements. The radiative and atomic phenomena, and particularly the flux, fluence, and spectrum of emitted radiation, obviously depend strongly on the fluid parameters, i.e. temperature/density profile, of the plasma.

This report discusses a recently developed numerical code, WHYRAC, which treats all of these phenomena in a fully self-consistent manner. WHYRAC represents a significant advance in flexibility, efficiency, and inclusion of more detailed physics over the first effort of this type[1]. WHYRAC is one-dimensional, permitting variation of macroscopic parameters only in the radial coordinate in cylindrical geometry. Thus it can treat either a single wire (possibly one of the wires in a multiple wire array)

Note: Manuscript submitted February 8, 1978.

as a Z-pinch, i.e. an axially symmetric plasma cylinder, confined by an azimuthal magnetic field driven by an axial current, or it can treat an array of wires mounted parallel to each other by representing the array as an azimuthally symmetric annulus. This report deals only with the physics and numerical techniques embodied in WHYRAC. Results from the code for specific physical problems and choices of parameters will be discussed in forthcoming reports.

WHYRAC is a significant advance over all previous efforts of this type. For the first time, the coupling of the wire plasma to the external circuit is treated in an exact, self-consistent way. Partially as a result of this, energy is conserved very accurately in the plasma/generator system. The code is modularized for extreme flexibility, both to handle a variety of situations and to permit continual upgrading of the physics. For example, the atomic physics/radiation package can use a perfect gas or other equation of state, coronal equilibrium, local thermodynamic equilibrium (L.T.E.), or more exact model, and presently includes a frequency-diffusion radiation transport model which can also be even further upgraded. The external circuit can be determined by specification of either a driving voltage V(t) or a circuit current I(t). The transport coefficients can easily be changed, in a way that is consistent throughout the code, e.g. various forms of anomalous resistivity can be specified, even if they depend self-consistently on a variety of plasma and circuit characteristics. Many of the choices made in writing the code, which will be discussed below, can be traced back to this requirement of flexibility.

The report is divided into three main parts. The first one reports the MHD equations to be solved and some of the problems associated with

their solutions. The second part describes the external circuit equations how they are solved self-consistently with the MHD equations. The third section discusses the atomic physics and radiation transport part of the code. Although it does not describe any atomic physics and radiation package in detail, it shows how the coupling is made to the rest of the code and along which lines the modularization takes place. A more detailed description of the atomic physics code will appear elsewhere.

II. The MHD Equations

The MHD equations are well-known and can be found in many textbooks.[2] They are presented here mainly for the sake of completeness. The equations describe the time evolution of a single fluid, two-temperature quasi-neutral plasma. The local ratio of electron to ion density, n_e/n_i, is equal to the mean ionization state $Z(r,t)$, determined by the atomic physics package. The continuity and momentum equations in cylindrical geometry are

$$\frac{\partial \rho}{\partial t} + \frac{1}{r} \frac{\partial}{\partial r} (r\rho v) = 0 , \tag{1}$$

$$\frac{\partial}{\partial t} (\rho v) + \frac{1}{r} \frac{\partial}{\partial r} (r\rho v^2) = - \frac{\partial p}{\partial r} + \frac{jB}{c} \tag{2}$$

where ρ is the mass density, v is the radial fluid velocity, j is the (axial) current density, B is the (azimuthal) magnetic field, and p is the total pressure (electrons + ions).

WHYRAC is a two-temperature code, but the electron and ion temperatures T_e and T_i are treated in a non-parallel way numerically. The two primary quantities that are solved for are T_e and the total plasma energy density E, defined by

$$E = \frac{1}{2}\rho v^2 + \frac{n_e kT_e}{(\gamma-1)} + \frac{3}{2} n_i kT_i . \tag{3}$$

The electron energy term $n_e kT_e/(\gamma-1)$ includes the potential energy of ionization. The effective adiabatic index γ, including these contributions, is calculated in the atomic physics package and discussed in Section IV. The two "energy" equations then read:

$$\frac{\partial E}{\partial t} + \frac{1}{r}\frac{\partial}{\partial r} r\left[(E + p)\, v + q_e\right] = j \cdot \mathcal{E} + P_{rad} \tag{4a}$$

$$\frac{1}{(\gamma-1)}\frac{\partial T_e}{\partial t} + \frac{1}{(\gamma-1}\, v\, \frac{\partial T_e}{\partial r} + \frac{P_e \frac{1}{r}\frac{\partial}{\partial r}(rv) + \frac{1}{r}\frac{\partial}{\partial r}(rq_e)}{n_e} = \frac{Q_e}{n_e} + \frac{P_{rad}}{n_e} \tag{4b}$$

where q_e is the total heat flux, $q_e = -K_{e\perp}\frac{\partial T_e}{\partial r} + \beta_\Lambda \left(\frac{\underline{B}}{|B|} \times \underline{u}\right)$,

$\mathcal{E}$ is the longitudinal electric field, $Q_e = j\left(\mathcal{E} - \frac{v_r B}{c}\right) + \alpha(T_i - T_e)$, and u is the (axial) current flow speed, defined by $j = -en_e u$, and P_{rad} is the radiative loss power. The transport coefficients $K_{e\perp}$, α, and β_Λ are given by Braginskii[2], in terms of various coefficients γ, δ, β which he tabulates:

$$K_{e\perp} = \frac{n_e T_e \tau_e}{m_e} \frac{\gamma_1' (\omega_e\tau_e)^2 + \gamma_o'}{(\omega_e\tau_e)^4 + \delta_1(\omega_e\tau_e)^2 + \delta_o} , \tag{5a}$$

$$\alpha = + \frac{3m_e}{m_i}\frac{n_e}{\tau_{ei}} , \tag{5b}$$

$$\beta_\wedge = n_e T_e \frac{\omega_e\tau_e \left[\beta_1''(\omega_e\tau_e)^2 + \beta_o''\right]}{(\omega_e\tau_e)^4 + \delta_1(\omega_e\tau_e)^2 + \delta_o} \quad . \tag{5c}$$

Ion heat conduction (generally small) was neglected in Eq. (4b). T_i and p are treated as secondary quantities. The former is obtained from Eq. (3), while the latter is obtained by using T_e, T_i, n_e and n_i in an equation of state (perfect gas is used), where n_e is calculated in the atomic physics package described in Section 4.

This numerical treatment affords great accuracy in overall energy conservation[3], and accurate calculation of T_e, which is a controlling parameter in many sensitive areas of the code, e.g. evolution of atomic states, radiation emission, resistivity. T_i is not always calculated with great accuracy, but this is not a significant deficiency, since T_i is only needed as a diagnostic and does not appear directly in the equations of evolution.

The extra equation describing the diffusion of the magnetic field, derived from the generalized Ohm's law, is

$$\frac{\partial B}{\partial t} = -\frac{\partial}{\partial r}(vB) + \frac{c^2}{4\pi}\frac{\partial}{\partial r}\frac{\eta_\perp}{r}\frac{\partial}{\partial r} rB + \frac{c}{e}\frac{\partial}{\partial r}\frac{\beta_\wedge}{n_e}\frac{\partial T_e}{\partial r} \quad . \tag{6a}$$

where $\eta_\perp$ is the (cross-field) resistivity, whose classical value[2] is

$$\eta_\perp = 1.13\ 10^{-14}\ Z\ \ln\Lambda\ T_{e_{eV}}^{-\frac{3}{2}} \tag{6b}$$

The current density profile j(r) is then determined from Faraday's law, $\frac{1}{r}\frac{\partial}{\partial r} rB(r) = \frac{4\pi}{c} j(r)$.

The explicit flux-corrected transport (FCT) algorithm[4] was used to solve Equations (1)-(5) numerically, with the exception of the diffusion terms. Those terms plus Eq. (6) were solved using an implicit tridiagonal solver. In the heat-diffusion term q_e, the thermo-electric term $\beta_\Lambda \left(\frac{B}{|B|} \times \underline{u}\right)$, was removed and solved with the convective terms. In fact, the change in the energy density due to that term in Eq. (4) is given by:

$$\frac{\partial E}{\partial t} + \frac{1}{r} \frac{\partial}{\partial r} r \beta_\Lambda u = 0 \tag{7}$$

In this equation, β_Λ is of the form $\beta_\Lambda \equiv n_e k T_e f(\omega_e \tau_e)$. Thus, the thermo-electric term looks like a convective term and can be solved for explicitly on the same time scale as the fluid convective terms provided that:

a) u is not larger than the maximum velocity used in the Courant criterion ($|v| + c_s$).

b) $f(\omega_e \tau_e)$ is of order 1.

We shall see that u does not go much above c_s in the course of the calculation, where c_s is the ion acoustic speed. Also, $f(\omega_e \tau_e)$ is shown in Figure 1 and reaches a maximum of 0.53 at $\omega_e \tau_e = 0.12$. The thermo-electric term then does not add any extra restrictions on the fluid time step and can be included in an explicit calculation like the one used for the convective terms.

The equilibration term between electrons and ions in Eq. (6) might also be a source of time-step problems. At the beginning of the run, the plasma is cold and the electron-ion equilibration time can be quite short, compared to the time step specified by other requirements. In order not to be limited by this short equilibration time, we follow a

treatment similar to that one used by Christiansen and Roberts.[5] Let us write this term in the following way

$$\frac{\partial T_e}{\partial t} = \frac{T_i - T_e}{\tau_1} \quad \text{with } \tau_1 = \frac{m_i \tau_{ei}}{3(\gamma-1)m_e} \tag{8}$$

where γ is the adiabatic index for the electron thermal plus atomic excitation and ionization energy, discussed in Sec. 4. The equilibration time τ_1 can become much smaller than the hydrodynamic time step δt (defined by the Courant condition), and we define $\Delta T = T_e - T_i$. The previous equation can be written

$$\frac{\partial \Delta T}{\partial t} = - \frac{\Delta T}{\tau_2} \quad \text{where } \tau_2 = \tau_1 \Big/ \left(1 + \frac{2}{3} \frac{Z}{(\gamma-1)}\right) \tag{9}$$

with the solution

$$\Delta T = (\Delta T)_{old} \, e^{-\delta t/\tau_2} \tag{10}$$

Going back to the original variable yields

$$T_e = (T_e)_{old} \, e^{-\delta t/\tau_2} + (T_i)_{old} \, (1 - e^{-\delta t/\tau_2}) \tag{11}$$

Thus far, the discussion has been quite general and applicable to any MHD problem. At this point, we discuss some of the physics associated specifically with exploding wire and Z-pinch problems.

Since a region of perfect vacuum cannot be maintained in an Eulerian fluid code, we legislate a minimum density for the gas surrounding the Z-pinch, i.e. whenever the density falls below some arbitrarily chosen value ρ_{min} in any given cell, additional mass is introduced to raise ρ to ρ_{min}. Typically we choose ρ_{min} to be 10^{-4} of the initial peak density, but other choices can be made instead. This standard technique

does not cause significant errors in mass conservation, but other types of difficulties do occur in treating the MHD of the low density regions, including the following.

According to the classical resistivity formula (5d), the resistivity is essentially independent of density (for a fully ionized gas), and thus can be very small in a hot, low density region. If the resistivity is small, the current tends to flow at the outside of the conducting region (skin effect). Thus a vicious circle occurs, with the current flowing exclusively at the outside of the low density ($\rho = \rho_{min}$) region (rather than in the region occupied by the Z-pinch in a real experiment), and heating this low density plasma to further reduce the local resistivity.

In real life, the resistivity in low density regions becomes anomalously high, because of plasma instabilities, thus allowing the current to penetrate to higher density regions. Marginal stability calculations[8,9] have shown that the exact value of the anomalous transport coefficients do not control the physics in this regime; rather, it is the turn-on condition for instability to occur that is crucial. In this spirit, we include an anomalous resistivity of the arbitrarily chosen form

$$\eta_{anom} = \eta_{class} \times \text{Max}\,[100,\ (u/c_s)^2], \tag{12}$$

whenever $u^2 > c_s^2 \equiv (Z\,T_e + T_i)/m_i$. This prescription has the effect of limiting the electron drift speed u to close to the ion sound speed c_s. We would note, however, that we believe that a much more sophisticated treatment of anomalous resistivity, based on detailed study of the relevant plasma instabilities, will be needed to explain some aspects of

wire phenomena. It is our intention to pursue these aspects of the physics and to continue to upgrade the code here.

In addition to the inclusion of anomalous resistivity, it is sometimes necessary to legislate that current may flow only in regions where $\rho \geq \rho_c$, where ρ_c is chosen to be larger than ρ_{min} by some arbitrarily chosen factor. Whenever this is done, the results are checked to insure that they do not depend significantly on the choice of ρ_c.

Numerical difficulties also arise because the Alfven speed can become very large in the low density region, as the current, and therefore B, increases. As a result, the time step (chosen to satisfy the Courant condition) can become intolerably small. This difficulty is avoided by adding a term $B^2/4\pi c_1^2$ to the inertia in the low-density region, thereby reducing the effective Alfven speed[6,7]. The quantity c_1 is varied with time to insure that the Alfven time scale (which is really an artifact of the density floor in the code) is no faster than the true hydrodynamic time scale. Of course, it is important to make sure that this correction is made only in regions where the density is lower than the density range of physical interest.

III. CIRCUIT EQUATION

The external circuit (pulse power generator plus diode) is modeled in the code as a driving voltage $V_g(t)$ into an effective lumped circuit with resistance Z_g and inductance L_g. The wire plasma, however, is treated in an exact way as a distributed circuit element, thus permitting an accurate evaluation of the energy coupled into the plasma. Our circuit equation is then

$$V_g(t) = Z_g\, I + L_g\, \frac{dI}{dt} + V_{p\ell}\ , \tag{13}$$

where $V_{p\ell}$ is the voltage across the plasma, which is calculated by a generalization of the method used in Refs. 10. The wire plasma in its return current cage is modeled as a plasma cylinder or annulus, in contact at one end with a grounded perfectly conducting metal return current path, and at the other end with an electrode at voltage $V_{p\ell}(t)$, as shown in Fig. 2. We then draw an imaginary current loop along the plasma at radius r, through the perfectly conducting return current path, and across the gap at $Z = \ell$, as shown in Fig. 2, and integrate Faraday's equation

$$\nabla \times \underline{\mathcal{E}} = \frac{1}{c}\, \frac{\partial \underline{B}}{\partial t} \tag{14}$$

across the loop. We then write down the generalized Ohm's law,

$$\underline{\mathcal{E}} + \frac{\underline{v}\times\underline{B}}{c} + \frac{1}{n_e e}\left(\nabla P_e - \frac{m_e Z}{m_i}\nabla_{Pi} + \beta_\perp \nabla_\perp T_e + \beta_\Lambda\, \frac{\underline{B}}{|B|} \times \nabla T_e - \frac{\underline{j}\times\underline{B}}{c}\right) = \eta_\perp\, j\ , \tag{15}$$

where $\underline{\mathcal{E}}$ is the electric field, p_e the electron pressure, p_i the ion pressure and the β's are defined as in ref. 2.

From Eq. (15) we note the following two useful consequences. First, from the axial component of Eq. (15), $\int dz\ \mathcal{E}_z(r,z) = \eta_\perp(r) j(r) \ell - \frac{v(r)B(r)\ell}{c} + \frac{\mathcal{E}_t \ell}{c}$, where $\mathcal{E}_t \equiv \beta_\Lambda \nabla T_e$ is the thermo-electric field. Second, the radial component of Eq. (15) shows that radial potential drops $\int_{r_1}^{r_2} dr\ \mathcal{E}_r(r,z)$ are of the order of T_e <u>within the plasma</u> (i.e. few

kilovolts at most), and therefore are very small compared to axial potential drops (of order few x 10^5 eV to few MeV). This is true even through the radial electric fields can be large, if the plasma cylinder is narrow. It follows that the current loop of Eq. (14) can be taken at any radial position within the plasma. The integrated form of Eq. (14) is thus

$$V_{p\ell} = \eta(r) j(r) \ell - \frac{v(r) B(r) \ell}{c} + \frac{\mathcal{E}_t \ell}{c} + \frac{\ell}{c} \int_r^{r_w} dr' \frac{\partial}{\partial t} B(r', t), \qquad (16)$$

where r_w is the wall radius and r is any location within the plasma. Note that the four terms on the right hand side of Eq. (16) play the role of resistive, L, thermoelectric and inductive circuit elements, but that it is impossible to perform this decomposition into lumped circuit elements until the current distribution is known, i.e. the circuit problem is solved.

It is clear that, in general, the self-consistent solution to Eqs. (6, 13, 16) can be obtained only by iterations since $V_{p\ell}$, I and B(r) are all coupled. $V_{p\ell}$ is needed to calculate I from Eq. (13), the radial profile of j or B is needed to calculate $V_{p\ell}$ from Eq. (16), while I is needed as a boundary condition in Eq. (6) to calculate B (r). However, if we take for r the value corresponding to the cell location from which the current stops flowing by convention (and denoting this value by r_c), the integral in Eq. (16) can be expressed in term of I. If in addition, we are satisfied with first-order accuracy in time (the overall accuracy of the code), Eq. (16) can be written

$$V_{p\ell} = \ell \mathcal{E}_z^o (r_c) + \frac{2\ell}{c^2} \int_{r_c}^{r_w} \frac{\partial I}{\partial t} \frac{\partial r'}{r'} \qquad (17)$$

where $\mathcal{E}_z^o (r_c)$ is the old value of the electric field at that point. Substituting this value in Eq. (13), it becomes

$$\left(L_g + \frac{2\ell}{c^2} \ell n \frac{r_w}{r_c}\right) \frac{\partial I}{\partial t} + Z_g I = V_g - \ell \mathcal{E}_z^o (r_c) \qquad (18)$$

The iterations are not needed anymore because the B-field has been expressed as a function of I.

It remains to calculate the local electric field, in order to determine $\underline{\mathcal{E}} \cdot \underline{j}$ in the plasma energy equations as mentioned in the previous section. The most direct way to evaluate $\mathcal{E}$ is given by the axial component of the generalized Ohm's law, Eq. (15), which reads,

$$\mathcal{E} = \eta_\perp j - \frac{vB}{c} - \frac{\beta_\Lambda}{n_e} \frac{\partial T_e}{\partial r} \qquad (19)$$

However, use of this form in a numerical calculation can lead to a choppy electric field. For example, anomalous resistivity can introduce large differences from cell to cell. Also, low density cells present quite large variations in velocity and the second term might, in fact, lead to negative values for the electric field.

Another expression for $\mathcal{E}$, which is mathematically equivalent but far more satisfactory for numerical finite difference calculations, can be obtained directly from the B field. Eq. (16) can be rewritten as

$$V_{p\ell} = \mathcal{E}_z(r)\ \ell + \frac{\ell}{c}\int_{r}^{r_w} \frac{\partial}{\partial t}\ B\ dr' \ . \qquad (20)$$

Since $V_{p\ell}$ is the same everywhere in the plasma, $\mathcal{E}$ inside the plasma can be calculated from point to point starting with the value given in Eq. (19). $\mathcal{E}$ is then obtained directly as a function of the magnetic field flux and nothing else. B being the solution of a diffusion equation is expected to be smooth and $\mathcal{E}_z$ should reflect this property.

The electric field obtained this way, when multiplied by $\underline{j}$ (obtained from $\underline{j} = \frac{1}{4\pi}\nabla x\underline{B}$), represents the total electromagnetic energy going into the plasma, and should satisfy the conservation relation

$$\int IV_{p\ell}\ dt = \int\int \underline{\mathcal{E}} \cdot \underline{j}\ dVdt + \int \frac{B^2}{8\pi}\ dV \qquad (21)$$

Eq. (21) is satisfied to much better accuracy (of the order of a few %) when $\mathcal{E}$ is derived from the magnetic field flux, Eq. (20), than when it is obtained from Ohm's law, Eq. (19). For the latter, the energy check is satisfied only to within 50% after 1000 time steps. Also, in order to improve even further the accuracy of the current determination, the calculation was performed in two half time steps, in order to evaluate the contribution due to the I term

In the introduction, it was mentioned that either $V_g(t)$ or $I(t)$ could be used as input variables for the driving circuit. The above

description applies to the more complicated case when the generator voltage is specified. For a current-specified problem, the above procedure simplifies still further. The plasma voltage which was calculated in order to determine the current does not need to be calculated in this case (but still is evaluated for diagnostic purposes). Given the current, one can calculate the B field and the current density. In all cases, it is found that

$$\int j \, 2\pi r dr = I$$

is satisfied to very good precision.

IV. ATOMIC PHYSICS AND RADIATION

There are two very different motivations for computing the atomic and radiative behavior of the wire plasma as a function of time. First is our obvious interest in the flux, fluence, and detailed spectral characteristics of the x-radiation emitted from the plasma. Second is the feedback of energy sources and sinks associated with atomic excitation, ionization, and radiative transport on the hydrodynamic (temperature/density) evolution of the plasma. Very different types of atomic/radiative code packages are required to perform these two functions. The detailed calculation of emitted spectra is a diagnostic function, which may be carried out quite infrequently compared to the time step of the code, (as a post-processing facility, for example), but which deserves very detailed (and therefore slow running and costly) treatment of atomic physics and radiative transport. In our scheme, this is

accomplished by storing temperature/density profiles at any chosen time, for use as input to separate atomic/radiation codes which calculate detailed spectra. On the other hand, a much simpler and faster running atomic/radiation package is included in WHYRAC itself to accomplish the second function, i.e. to interface self-consistently with the energetics of the MHD and circuit packages in the code. This atomic/radiation package must run at every time step of the code, and thus depending on its complexity might constitute a large fraction of the running time of the code. It can be benchmarked against the more detailed diagnostic atomic/radiation codes to establish that its accuracy is sufficient unto its needs.

Our main purpose here is to discuss the general nature and interaction of the atomic/radiation section with the rest of the wire code, rather than to discuss the specifics of these atomic/radiation packages. This will be done in detail in subsequent reports, as the continual upgrading of accuracy and versatility (e.g. use for different elements) of these packages constitutes a major part of our exploding wire program.

We simply note that the atomic/radiation package presently being used in WHYRAC is an equilibrium model, in which one excited state is carried for each ionization stage, corresponding to the main transition line for that ionization level. Dielectronic recombination has also been included.[11] The treatment of radiation transport has been reduced to a local one. For each cell and for each line, an opacity is calculated corresponding to the shortest optical path out of the plasma. An escape probability is then calculated[12] and determines the fraction of the radiation which escapes the system and the fraction which remains in

that cell. The package needs as inputs only the total ion density and the electron temperature. The electron density, average Z, ionization energy and radiated power (frequency integrated or not) are all calculated within the atomic/radiation package.

Two problems, because of their possible impact on the rest of the code, have received special attention. One concerns the avoidance of negative temperatures due to radiation cooling, the other one the avoidance of too low a value of the adiabatic coefficient γ at low temperature.

The radiation cooling term is simply

$$\frac{\partial}{\partial t} \quad \frac{n_e k T_e}{(\gamma-1)} = - \; P_{rad}, \tag{22}$$

where P_{rad} is evaluated as part of the atomic physics package. Eq. (22) can be expanded into

$$\frac{\partial T_e}{\partial t} = - T_e \frac{1}{n_e} \frac{\partial n_e}{\partial t}\bigg|_i - \frac{1}{3/2 \; n_e k} \frac{\partial E_{chem}}{\partial t} - \frac{P_{rad}}{3/2 \; n_e k} \tag{23}$$

where $\frac{\partial n_e}{\partial t}\Big|_i$ is the rate of change of the electron density due to the changes in the ionization levels, E_{chem} is the potential energy of ionization (and, in general, atomic excitation). A problem can arise with the last term, if the change in temperature due to that term is to be evaluated in the hydrodynamic time step, since the P_{rad} term can become large enough to drive the temperature negative, for finite differencing on this time scale. This would really correspond to feeding energy into the code, since the temperature is reset to a minimum positive value whenever it goes negative. Physically, of course, the temperature does

not become negative because before hitting $T_e = 0$, the radiation cooling term would itself go to zero, so that the temperature evolution would really be like that one shown in Figure 3a. It is not possible to apply the same analysis as for the temperature equilibration term[5] discussed in Sec. 2, because there is no simple analytic solution to Eq. (23). A straightforward but sometimes very slow running approach would consist in splitting the hydro time step for that calculation, recalculating P_{rad} at each of this fractional time step and reaching small temperatures in a smooth fashion, as shown in Figure 3b. However, a much faster and still adequate way is to truncate the energy loss due to P_{rad} when T_e reaches a small value, at time interval δt^*. We then set T_e to that value and take $P_{rad}\, \delta t^*$ as the energy radiated in the time interval δt. This approach is shown in Figure 3c. Besides being very fast, it has the advantages of avoiding negative temperatures and also of not overestimating (in fact, underestimating somewhat) the radiated energy.

Another problem where the atomic physics impacts the hydrodynamics is the relative importance of the ionization energy E_{chem} in the internal energy. In the atomic physics part of the code, the ionization energy can be calculated. From that number, we define an effective adiabatic coefficient γ for the electron thermal plus ionization energy by

$$E_{chem} + \frac{3}{2} n_e kT_e = \frac{n_e kT_e}{(\gamma-1)} \qquad (24)$$

In this form, the electron internal energy represents the sum of the ionization and the electron thermal energy. When energy is added (or subtracted) to the plasma, a certain fraction is taken up by the ioni-

zation energy. As the temperature goes up, this fraction becomes smaller and smaller (γ then tends toward 5/3). At low temperatures, E_{chem} can be much larger than the thermal energy and leads to a value of γ very close to 1. This in turn leads to problems when division by (γ-1) occurs. A minimum γ is set up depending on the element in order to avoid this problem. (Incidentally, a correct approach to this problem would be to use a correct equation of state for the transition state between solid and plasma). The minimum value of γ is determined from the ionization energies of the first two levels. For example, for Al, the minimum value of γ used in the code is 1.134.

V. CONCLUSION

A new wire code WHYRAC has been developed. This code provides a new tool for the study of multiple-wire arrays, single wires, Z-pinches and other cylindrically symmetric plasma configurations. The code solves the circuit equations with the plasma included in a self-consistent way. No lumped electrical characteristics are used for the plasma in those equations. The atomic/radiation package has been designed to interact with the rest of the code in a standardized fashion and can be upgraded at will, depending on the amount of computation time which is to be spent in that stage. At this point of development of the code, a distinction is made between a fast "energetics" package and an elaborate diagnostic package which can be used as a post-processor for data generated by the code. As a last remark (in this numerically oriented report), the numerical "fixes" in the code have been kept to a minimum (and extensively discussed herein), and extensive tests have been made in order to

choose the most satisfactory algorithm to deal with each numerical problem and to minimize the effect of these choices on the physics.

ACKNOWLEDGMENT

This work was supported by the Defense Nuclear Agency under Subtask No. T99QAXLB202.

REFERENCES

1. D. Mosher, S. J. Stephanakis, K. Hain, C. M. Dozier and F. C. Young, Annals New York Academy of Science, 251, 632 (1975)
2. S. I. Braginskii in Reviews of Plasma Physics, edited by M. A. Leontovich (Consultants Bureau, New York, 1965), page 205.
3. D. G. Colombant and J. H. Gardner, J. Comp. Phys. 22, 389 (1976).
4. J. P. Boris and D. L. Book, J. Comp. Phys. 11, 38 (1973).
5. J. P. Christiansen and K. V. Roberts, J. Comp. Phys. 17, 332 (1975).
6. J. P. Boris, NRL Memorandum Report 2167, (1970). AD 715774.
7. D. V. Anderson, M. Lampe, and W. M. Manheimer, NRL Memorandum Report 2486 (1972). AD 748179.
8. M. Lampe, W. M. Manheimer, and K. Papadopoulous, NRL Memorandum Report 3076 (1975). AD A014411.
9. W. M. Manheimer and J. P. Boris, Comments Plasma Phys. Cont. Fusion 3, 15 (1977).
10. D. V. Anderson, M. Lampe, and W. M. Manheimer, NRL Memorandum Report 2486 (1972)AD 748179; W. M. Manheimer, Phys. Fluids 17, 1767 (1974).
11. V. L. Jacobs, J. Davis, P. C. Kepple and M. Blaha, Astro Phys. J. 211, 605 (1977).
12. P. Julienne and J. Davis, NRL Memorandum Report 2556 (1973). AD 907963L.

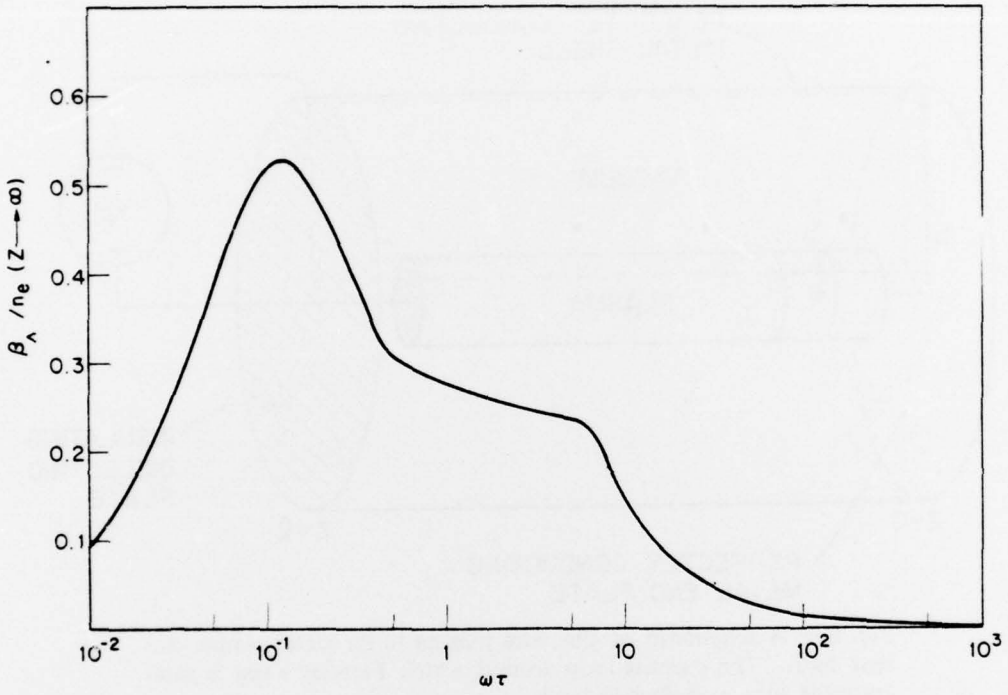

Fig. 1 — Variation of the thermo-electric term coefficient as a function of ($\omega\tau$)

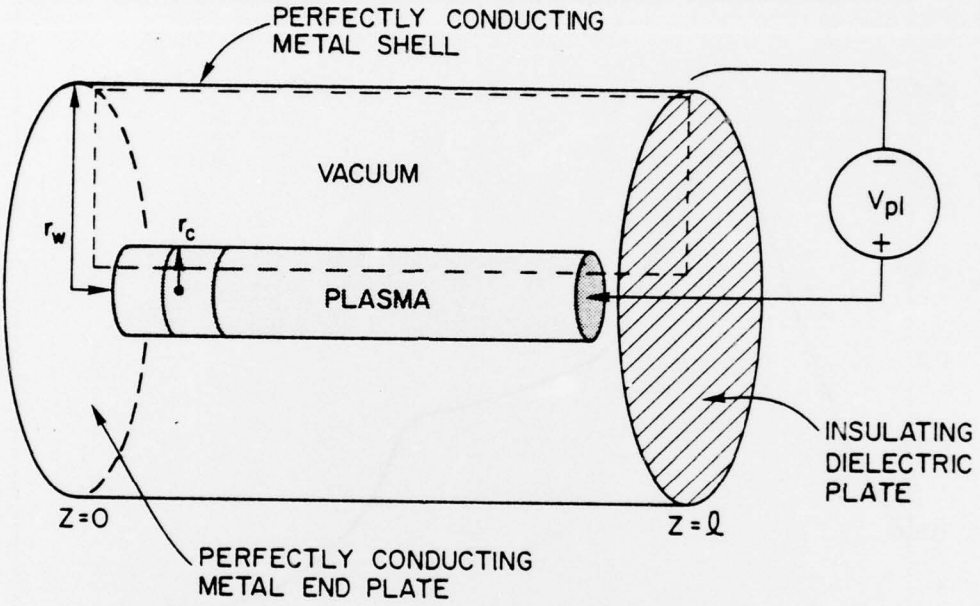

Fig. 2 — A schematic of the wire plasma in its metal return current path. The current loop around which Faraday's law is integrated is shown in dashed lines.

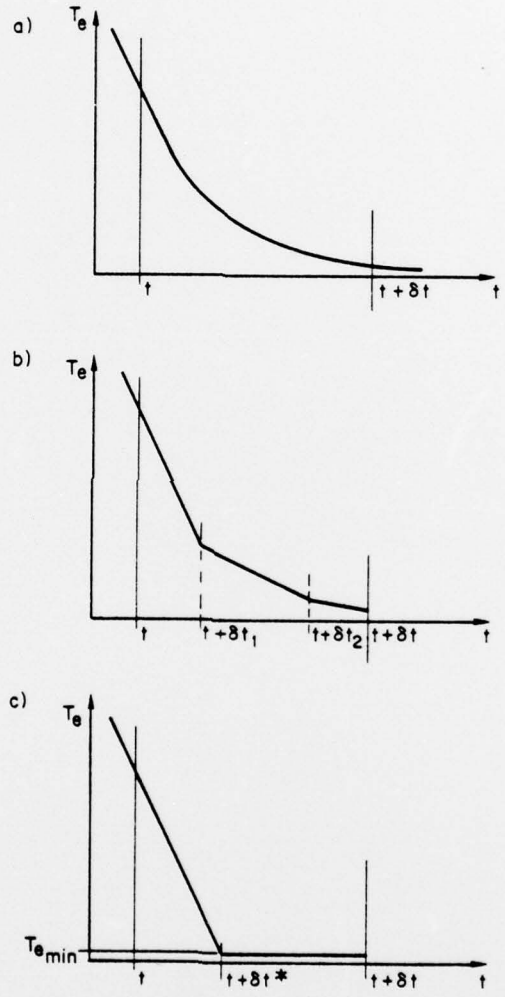

Fig. 3 — Variations of the local temperature as a function of time due to a large cooling radiative term: (a) in theory, (b) as could be implemented in a code and (c) as implemented in the code.

DNA DISTRIBUTION LIST

DEFENSE DOCUMENTATION CENTER
CAMERON STATION
ALEXANDRIA, VA 22314
(12 COPIES IF OPEN PUBLICATION, OTHERWISE 2 COPIES)
12 CY ATTN: TC

DIRECTOR
DEFENSE INTELLIGENCE AGENCY
WASHINGTON, DC 20301
1 CY ATTN: DTICI ROBERT I RUBENSTEIN

DIRECTOR
DEFENSE NUCLEAR AGENCY
WASHINGTON, DC 20305
1 CY ATTN: STVL
1 CY ATTN: TISI ARCHIVES
3 CY ATTN: TITL TECH LIBRARY
1 CY ATTN: RAEV

COMMANDER
FIELD COMMAND
DEFENSE NUCLEAR AGENCY
KIRKLAND AFB, NM 87115
1 CY ATTN: FCPR

DIRECTOR
JOINT STRAT TGT PLANNING STAFF JCS
OFFUTT AFB
OMAHA, NB 68113
1 CY ATTN: JSAS

CHIEF
LIVERMORE DIVISION FLD COMMAND DNA
LAWRENCE LIVERMORE LABORATORY
P.O. BOX 808
LIVERMORE, CA 94550
1 CY ATTN: FCPRL

UNDER SEC'Y OF DEF FOR RSCH & ENGRG
DEPARTMENT OF DEFENSE
WASHINGTON, DC 20301
1 CY ATTN: S&SS(OS)

COMMANDER
BMD SYSTEM COMMAND
P.O. BOX 1500
HUNTSVILLE, AL 35807
1 CY ATTN: SSC-TEN

DEP CHIEF OF STAFF FOR RSCH DEV & ACQ
DEPARTMENT OF THE ARMY
WASHINGTON, DC 20310
1 CY ATTN: DAMA-CSM-N

COMMANDER
HARRY DIAMOND LABORATORIES
2800 POWDER MILL ROAD
ADELPHI, MD 20783
(CNWDI-INNER ENVELOPE: ATTN: DELHD-RBH)
1 CY ATTN: DELHD-NP
1 CY ATTN: DELHD-RCC JOHN A. ROSADO
1 CY ATTN: DRXDO-RBH PAUL A. CALDWELL
1 CY ATTN: DRXDO-TI TECH LIB

COMMANDER
PICATINNY ARSENAL
DOVER, NJ 07801
1 CY ATTN: SMUPA ND-N-E

COMMANDER
REDSTONE SCIENTIFIC INFORMATION CTR
U.S. ARMY MISSILE COMMAND
REDSTONE ARSENAL, AL 35809
3 CY ATTN: CHIEF, DOCUMENTS

COMMANDER
U.S. ARMY MISSILE COMMAND
REDSTONE ARSENAL, AL 35809
1 CY ATTN: DRCPM-PE-EA

COMMANDER
U.S. ARMY NUCLEAR AGENCY
7500 BACKLICK ROAD
BUILDING 2073
SPRINGFIELD, VA 22150
1 CY ATTN: ATCN-W

COMMANDER
U.S. ARMY TEST AND EVALUATION COMD
ABERDEEN PROVING GROUND, MD 21005
1 CY ATTN: DRSTE-EL

CHIEF OF NAVAL OPERATIONS
NAVY DEPARTMENT
WASHINGTON, DC 20350
1 CY ATTN: ROBERT A. BLAISE 604C4

COMMANDER
NAVAL ELECTRONIC SYSTEMS COMMAND
NAVAL ELECTRONIC SYSTEMS CMD HQS
WASHINGTON, DC 20360
1 CY ATTN: CODE 5032

COMMANDING OFFICER
NAVAL INTELLIGENCE SUPPORT CTR
4301 SUITLAND ROAD BLDG. 5
WASHINGTON, DC 20390
1 CY ATTN: NISC-45

OFFICER-IN-CHARGE
NAVAL SURFACE WEAPONS CENTER
WHITE OAK, SILVER SPRING, MD 20910
1 CY ATTN: CODE WR43
1 CY ATTN: CODE WA501 NAVY NUC PRGMS OFF

COMMANDER
NAVAL WEAPONS CENTER
CHINA LAKE, CA 93555
1 CY ATTN: CODE 533 TECH LIB

AF WEAPONS LABORATORY, AFSC
KIRTLAND AFB, NM 87117
1 CY ATTN: CA
1 CY ATTN: ELC
1 CY ATTN: NT
1 CY ATTN: SUL
1 CY ATTN: DYP

HQ USAF/RD
WASHINGTON, DC 20330
1 CY ATTN: RDQSM

SAMSO/DY
POST OFFICE BOX 92960
WORLDWAY POSTAL CENTER
LOS ANGELES, CA 90009
(TECHNOLOGY)
1 CY ATTN: DYS

SAMSO/IN
POST OFFICE BOX 92960
WORLDWAY POSTAL CENTER
LOS ANGELES, CA 90009
1 CY ATTN: IND MAJ DARRYL S. MUSKIN

SAMSO/MN
NORTON AFB, CA 92409
(MINUTEMAN)
1 CY ATTN: MNNH

SAMSO/SK
POST OFFICE BOX 92960
WORLDWAY POSTAL CENTER
LOS ANGELES, CA 90009
(SPACE COMM SYSTEMS)
1 CY ATTN: SKF PETER H. STADLER

UNIVERSITY OF CALIFORNIA
LAWRENCE LIVERMORE LABORATORY
P.O. BOX 808
LIVERMORE, CA 94550
1 CY ATTN: L-18
1 CY ATTN: L-153
1 CY ATTN: JOHN NUCKOLLS A DIV L-545 (CLASS L-33)
1 CY ATTN: TECH INFO DEPT L-3

SANDIA LABORATORIES
P.O. BOX 5800
ALBUQUERQUE, NM 87115
1 CY ATTN: DOC CON FOR 3141 SANDIA RPT COLL
1 CY ATTN: DOC CON FOR 5240 GERALD YONAS

AVCO RESEARCH & SYSTEMS GROUP
201 LOWELL STREET
WILMINGTON, MA 01887
1 CY ATTN: RESEARCH LIB A830 RM 7201

BDM CORPORATION THE
7915 JONES BRANCH DRIVE
MCLEAN, VA 22101
1 CY ATTN: TECHNICAL LIBRARY

BOEING COMPANY, THE
P.O. BOX 3707
SEATTLE, WA 98124
1 CY ATTN: AEROSPACE LIBRARY

DIKEWOOD INDUSTRIES, INC.
1009 BRADBURY DRIVE, S.E.
ALBUQUERQUE, NM 87106
1 CY ATTN: L WAYNE DAVIS

EG&G, INC.
ALBUQUERQUE DIVISION
P.O. BOX 10218
ALBUQUERQUE, NM 87114
1 CY ATTN: TECHNICAL LIBRARY

FORD AEROSPACE & COMMUNICATIONS CORP
3939 FABIAN WAY
PALO ALTO, CA 94303
(FORMERLY AERONUTRONIC FORD CORPORATION)
1 CY ATTN: DONALD R. MCMORROW MS G30
1 CY ATTN: LIBRARY

FORD AEROSPACE & COMMUNICATIONS OPERATIONS
FORD & JAMBOREE ROADS
NEWPORT BEACH, CA 92663
(FORMERLY AERONUTRONIC FORD CORPORATION)
1 CY ATTN: TECH INFO SECTION

GENERAL ELECTRIC COMPANY
SPACE DIVISION
VALLEY FORGE SPACE CENTER
GODDARD BLVD KING OF PRUSSIA
P.O. BOX 8555
PHILADELPHIA, PA 19101
1 CY ATTN: JOSEPH C. PEDEN VFSC, RM 4230M

GENERAL ELECTRIC COMPANY
TEMPO-CENTER FOR ADVANCED STUDIES
816 STATE STREET, (P.O. DRAWER QQ)
SANTA BARBARA, CA 93102
1 CY ATTN: DASIAC

INSTITUTE FOR DEFENSE ANALYSES
400 ARMY-NAVY DRIVE
ARLINGTON, VA 22202
1 CY ATTN: IDA LIBRARIAN RUTH S. SMITH

ION PHYSICS CORPORATION
SOUTH BEFORD STREET
BURLINGTON, MA 01803
1 CY ATTN: H. MILDE

IRT CORPORATION
P.O. BOX 81087
SAN DIEGO, CA 92138
1 CY ATTN: R. L. MERTZ

JAYCOR
1401 CAMINO DEL MAR
DEL MAR, CA 92014
1 CY ATTN: ERIC P. WENAAS

JAYCOR
205 S. WHITING STREET, SUITE 500
ALEXANDRIA, VA 22304
1 CY ATTN: ROBERT SULLIVAN

KAMAN SCIENCES CORPORATION
P.O. BOX 7463
COLORADO SPRINGS, CO 80933
1 CY ATTN: ALBERT P. BRIDGES
1 CY ATTN: JOHN R. HOFFMAN
1 CY ATTN: DONALD H. BRYCE
1 CY ATTN: WALTER E. WARE

LOCKHEED MISSILES AND SPACE CO INC
3251 HANOVER STREET
PALO ALTO, CA 94304
1 CY ATTN: LLOYD F. CHASE

MAXWELL LABORATORIES, INC.
9244 BALBOA AVENUE
SAN DIEGO, CA 92123
1 CY ATTN: A. RICHARD MILLER
1 CY ATTN: PETER KORN
1 CY ATTN: Wayne Clark

MCDONNELL DOUGLAS CORPORATION
5301 BOLSA AVENUE
HUNTINGTON BEACH, CA 92647
1 CY ATTN: STANLEY SCHNEIDER

MISSION RESEARCH CORPORATION
735 STATE STREET
SANTA BARBARA, CA 93101
1 CY ATTN: WILLIAM C. HART
1 CY ATTN: CONRAD L. LONGMIRE

MISSION RESEARCH CORPORATION-SAN DIEGO
P.O. BOX 1209
LA JOLLA, CA 92038
(VICTOR A. J. VAN LINT)
1 CY ATTN: V. A. J. VAN LINT

NORTHROP CORPORATION
NORTHROP RESEARCH AND TECHNOLOGY CTR
3401 WEST BROADWAY
HAWTHORNE, CA 90250
(DESIRES ONLY 1 COPY OF CNWDI MAT)
1 CY ATTN: LIBRARY

NORTHROP CORPORATION
ELECTRONIC DIVISION
2301 WEST 120TH STREET
HAWTHORNE, CA 90250
1 CY ATTN: VINCENT R. DEMARTINO

PHYSICS INTERNATIONAL COMPANY
2700 MERCED STREET
SAN LEANDRO, CA 94577
1 CY ATTN: DOC CON FOR BERNARD H. BERNSTEIN
1 CY ATTN: DOC CON FOR CHARLES H. STALLINGS
1 CY ATTN: DOC CON FOR PHILIP W. SPENCE
1 CY ATTN: DOC CON FOR Bernie Lippmann
1 CY ATTN: DOC CON FOR SIDNEY D. PUTNAM

PULSAR ASSOCIATES, INC.
11491 SORRENTO VALLEY BLVD
SAN DIEGO, CA 92121
1 CY ATTN: CARLETON H. JONES JR.

R & D ASSOCIATES
P.O. BOX 9695
MARINA DEL REY, CA 90291
1 CY ATTN: C. MACDONALD
1 CY ATTN: WILLIAM R. GRAHAM JR.
1 CY ATTN: LEONARD SCHLESSINGER

SCIENCE APPLICATIONS, INC.
P.O. BOX 2351
LA JOLLA, CA 92038
1 CY ATTN: J. ROBERT BEYSTER

SPIRE CORPORATION
P.O. BOX D
BEDFORD, MA 01730
1 CY ATTN: ROGER G. LITTLE

SRI INTERNATIONAL
333 RAVENSWOOD AVENUE
MENLO PARK, CA 94025
1 CY ATTN: SETSUO DDAIRIKI

SYSTEMS, SCIENCE AND SOFTWARE, INC.
P.O. BOX 4803
HAYWARD, CA 94540
1 CY ATTN: DAVID A. MESKAN

SYSTEMS, SCIENCE AND SOFTWARE, INC.
P.O. BOX 1620
LA JOLLA, CA 92038
1 CY ATTN: ANDREW R. WILSON

TEXAS TECH UNIVERSITY
P.O. BOX 5404 NORTH COLLEGE STATION
LUBBOCK, TX 79417
1 CY ATTN: TRAVIS L. SIMPSON

TRW DEFENSE & SPACE SYS GROUP
ONE SPACE PARK
REDONDO BEACH, CA 90278
1 CY ATTN: TECH INFO CENTER/S-1930

VOUGHT CORPORATION
MICHIGAN DIVISION
38111 VAN DYKE ROAD
STERLING HEIGHTS, MI 48077
(FORMERLY LTV AEROSPACE CORPORATION)
1 CY ATTN: TECH LIB

NRL CODE 2628 - 20 CYS

NRL CODE 6700 - 1 CY

NRL CODE 6750 - 20 CYS (1 CY CLASSIFIED)